The Geodynamo

D R Fearn

August 19, 2004

1 The Earth and its magnetic field

1.1 A brief history

Interest in the Earth's magnetic field goes back some 2000 years, in particular to the ancient Chinese, whose major achievements include the invention of the magnetic compass and the subsequent discovery of *declination*, the angle between magnetic and geographic north. Initially, the compass was believed to be attracted to the pole star. Later, the favoured source of attraction moved to the polar regions of the Earth and subsequently to the interior of the Earth. This followed the discovery in Europe in the 16^{th} Century of *inclination*, the angle of dip of the field direction. At this time, considerable effort was expended in mapping the declination and inclination as a potential aid to navigation. Modern maps can be found at "`http://geomag.usgs.gov/`". The year 2000 was the 400^{th} anniversary of William Gilbert's treatise on geomagnetism *De Magnete*. This gave the first rational explanation for the mysterious ability of the compass needle to point north-south; that the Earth itself was magnetic.

Up until this point, the Earth's magnetic field had been assumed to be steady, but it was not long before a series of observations at Greenwich led Henry Gellibrand in 1634 to deduce that the declination changes with time. This was the first observed feature of the so-called *Geomagnetic Secular Variation* (GSV), the slow (on a human time scale) change of the field emanating from the Earth's core. From detailed observations we now know this behaviour in considerable detail over the past few hundred years (see for example Courtillot & Le Mouël, 1988; Bloxham & Jackson, 1992; Jackson *et al.* 2000).

Much further information about the Earth's field and its history can be found at the de Magnete website at "`http://www-spof.gsfc.nasa.gov/earthmag/demagint.htm`", see also Chapter 1 of Merrill *et al.* (1996) and Stern (2002).

1.2 Structure of the Earth

A spherical harmonic analysis of the geomagnetic field averaged over a few years shows clearly that the long-time field is essentially entirely of internal origin (see for example the discussion in Backus *et al.* 1996). A key prerequisite to understanding the generation

Figure 1: The interior of the Earth.

mechanism of the field is therefore a knowledge of the interior of the Earth. Our principal sources of information are: (A) the composition of meteorites thought to be characteristic of the material from which the Earth was formed, (B) the analysis of seismic waves, and (C) the properties of materials at high pressure determined from high-pressure experiments and, more recently, theoretical calculations. Useful references, explaining the ideas, are Bolt (1982), Melchior (1986), Stacey (1992) and Poirier (2000). A review of the theoretical approach can be found in Alfè *et al.* (2002b).

These three sources give the following picture, see Figure 1. The Earth is composed of a core of radius 3485 km surrounded by a rocky mantle of radius 6370 km. On top of that is the thin crust on which we live. The mantle is a good electrical insulator (except perhaps close to its boundary with the core) so the only possible source of electromagnetic induction that can generate magnetic field is in the core. The core has two distinct parts: an *inner core* of radius 1215 km that is solid and an *outer core* that is fluid. The principal constituent of both is iron. While the density of the inner core is consistent with it being pure iron, the density of the outer core is up to 10% lighter than iron at core pressures. While there remains considerable controversy as to the identity of the lighter element or elements that are mixed with iron in the outer core, it is clear that the outer core is composed of a mixture of iron and some lighter constituents. Possible candidates include sulphur, oxygen and silicon. Recent studies have estimated the core density deficit at closer to 5% (Anderson & Isaac 2002) and have highlighted the importance of oxygen in the core (Alfè *et al.* 2002a).

The presence of the solid inner core can be explained by the freezing of the outer core. While the temperature in the interior of the Earth increases with depth, the freezing temperature also increases because of the effect of pressure. Indeed, the latter increases more rapidly with depth. This explains why, as the Earth cools, freezing takes place first

at the centre. It is believed that the core was initially completely molten and that a proto inner core nucleated first at the centre of the Earth several billion years ago and has grown steadily since then through the freezing of the outer core. Estimates of the age of the inner core vary. Recent studies put it as at least 3 Gyr (1GYr = 10^9 years) to explain the paleomagnetic measurements of the Earth's field, see Gubbins *et al.* (2003, 2004) but, for example, Labrosse *et al.* (2001) estimate it at 1 Gyr based on the assumption of no radioactive heating in the core. See also Roberts *et al.* (2001) who come to a similar conclusion but then go on to consider the consequences of all the potassium 40 "missing" from the Earth being in the core (see Section 1.4).

It is a common property of mixtures that the composition of the solid which freezes is different from that of the fluid from which it has frozen. For example, if sea water is cooled, the ice that forms contains very little salt, with the remaining fluid being enriched in salt. The same process is believed to take place as the outer core fluid freezes; as the mixture of iron and lighter constituent cools, what freezes is predominantly iron, with most of the light constituent being rejected into the remaining outer core. This explains the observed density contrast between the inner and outer cores which is larger than can be explained by density change upon freezing. Our picture then is of a dense inner core growing steadily as the Earth cools, with the density of the remaining outer core gradually decreasing as the fraction of light constituent in it increases. This picture has major implications for the energy source of the geodynamo which we discuss in Section 1.4.

1.3 The geomagnetic field

While direct measurements of the Earth's field go back only a few hundred years, we have information on its behaviour going back several billion years through *paleomagnetic* measurements, see for example Merrill *et al.* (1996). Though most rock forming minerals are non-magnetic, all rocks exhibit some magnetic properties due to the presence of traces of iron oxides. The magnetisation of these may be used to determine both the local direction and intensity of the Earth's field at the time the rock was formed. Relatively short time-scale behaviour can be determined from sequences of lava flows, and longer time-scale behaviour from sedimentary rocks.

Intensity measurements show that the field has roughly maintained its strength over the past 3.5 GYr, see Figure 2. When compared with the ohmic decay time of the Earth's core

$$\tau_\eta = \frac{r_o^2}{\eta} \approx 3 \times 10^5 \text{ years}, \tag{1}$$

there is a clear requirement to explain how the field is maintained and what is its energy source. Permanent magnetism is not a possible explanation because, below a depth of the order of a hundred kilometers, the temperature inside the Earth exceeds the Curie temperature (see for example Stacey 1992). In (1), r_o is the radius of the core and $\eta = 1/\mu\sigma$ is the magnetic diffusivity of the core, μ is the magnetic permeability (usually taken to be the free-space value $\mu_0 = 4\pi \times 10^{-7}$ Hm^{-1}) and σ is the electrical conductivity. For the

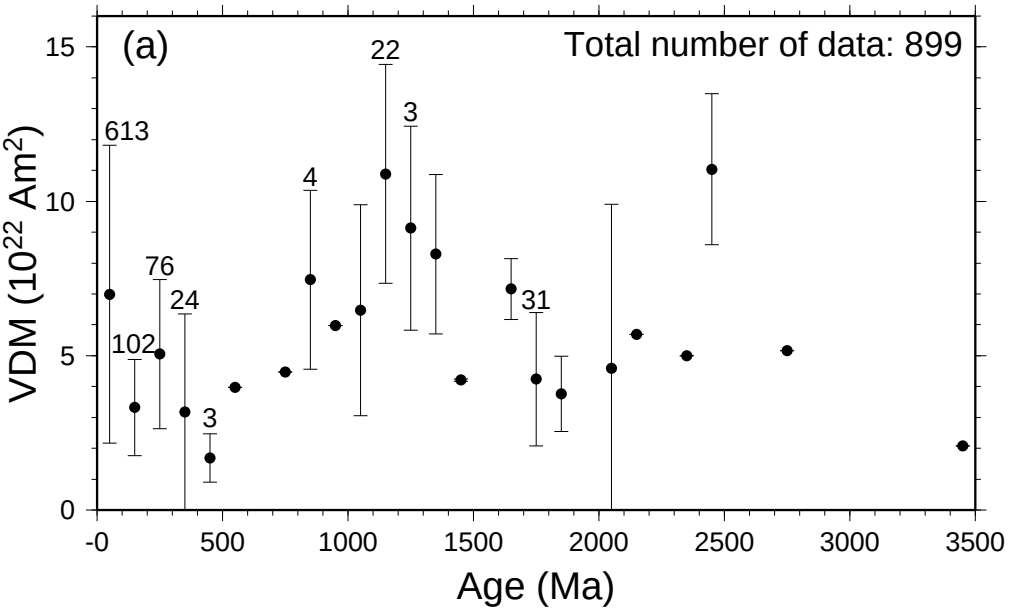

Figure 2: Intensity of the geomagnetic field over the past 3.5Gyr averaged over 100Myr intervals. The current strength is 8×10^{22} Am^2. From Kono & Tanaka (1995).

Earth, substituting $r_o = 3.485 \times 10^6$ m and $\sigma \approx 6 \times 10^5$ Sm^{-1} (Merrill *et al.* 1996) gives $\eta \approx 1.3$ m^{2}s^{-1}.

The principal component of the Earth's field at present is a dipole whose axis is roughly aligned with the geographic axis (the declination measuring the deviation). Indeed, the average field over the past 5MYr closely approximates a geocentric axial dipole (see Merrill & McFadden 2003). Directional paleomagnetic measurements show that the field has reversed its direction many times. Reversals are irregular and take place over a time that is short (of the order of 5000 years) compared with the quiescent period between reversals. The last (the Brunhes-Mutuyama reversal) was some 7×10^5 years ago. The reversal frequency has varied over time, see Figure 3 and McFadden & Merrill (2000). Typically there have been a few every million years over the past 45 Myr but there was a period (the Cretaceous Superchron) of some 20 Myr ending 86 Myr ago in which hardly any reversals have been found (see Merrill *et al.* 1996). Heller *et al.* (2002) have investigated the relationship between the frequency of reversals and what is known about the field intensity. They conclude "that there is not a simple correlation between reversal rate and intensity". In addition to reversals, features known as *excursions* have been found. When observed in detail, these start off in a similar way to reversals, with an increase in the declination and typically a decrease in intensity. However, in these events, the field returns to its original polarity rather than the reversed one. Excursions may be "aborted reversals" and may occur ten times more frequently than reversals, see for example Gubbins (1999). They may be due to an intrinsic instability of the dynamo process, see McFadden & Merrill (1993) and Zhang & Gubbins (2000). McFadden & Merrill demonstrate that, following a reversal, there is a reduced probability of a further reversal during a period of some 45000

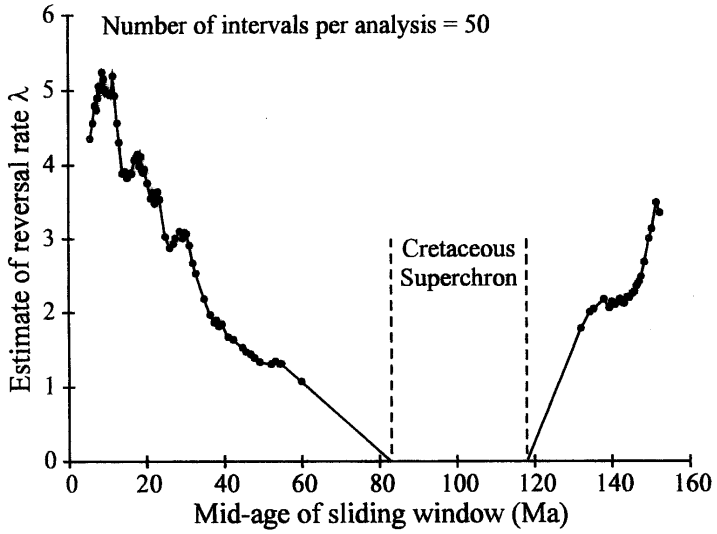

Figure 3: Frequency of reversal of the Earth's magnetic field. From Merrill *et al.* (1996). The vertical scale indicates the number of reversals per MYr.

yrs, a period of the order of τ_η.

The governing equations (4a)-(4d) clearly admit $-\mathbf{B}$ as a solution if $\mathbf{B}$ is a solution, so the existence of reversed fields is not a puzzle. However, we do not have a good understanding of what triggers a reversal, what influences their frequency or why some should fail. Simulations are beginning to give some insight into these issues, see Section 5. For example, the pattern of heat flux at the CMB has been shown to strongly influence reversal behaviour (Glatzmaier *et al.* 1999), see Figure 5

1.4 Energy sources

The observation in the previous section that the Earth's field has existed at around its present strength for a time four orders of magnitude longer than the ohmic diffusion time (1) clearly indicates the need for a mechanism for maintaining the field against ohmic decay, together with an adequate power source. A rough estimate of the power required can be obtained by setting $\mathbf{u} = 0$ in (4a), taking the scalar product with $\mathbf{B}/\mu_0$ and integrating over all space V to give

$$P = \frac{d}{dt}\int_V \frac{\mathbf{B}^2}{2\mu_0} dV = -\int_V \frac{\mathbf{J}^2}{\sigma} dV \tag{2}$$

The standard vector identity (**??**) and the divergence theorem have been used in deriving (2). For an insulating mantle, the current $\mathbf{J}$ vanishes outside the core. The left-hand side of (2) is the rate of change of magnetic energy. Now, since $\mu_0\mathbf{J} = \boldsymbol{\nabla}\times\mathbf{B}$, the ohmic power dissipation can then be roughly estimated from the right-hand side to give

$$P \approx \frac{4}{3}\pi r_o^3 \frac{\mathcal{B}^2}{\sigma\mu_0^2\mathcal{L}^2}, \tag{3}$$

where $\mathcal{B}$ is a typical field strength and $\mathcal{L}$ an appropriate length scale (which cannot be greater than r_o). If we choose $\mathcal{L} = 10^6$ m, then (3) gives an ohmic power dissipation of $1.4 \times 10^{14}\mathcal{B}^2$ W. For a field strength of 6 mT this equates to 5×10^9W. Of course, this estimate depends crucially on our (rather arbitrary) choice of $\mathcal{L}$. Shorter length scales lead to higher dissipation. Loper and Roberts (1983) reviewed the various estimates; these give $P/\mathcal{B}^2$ in the range from 0.7×10^{14} to 200×10^{14}WT^{-2}. Loper and Roberts (1983) favour a value, somewhere in the middle of this range, of $P/\mathcal{B}^2 = O(10^{15})$WT^{-2}. A field of 10 mT then requires $O(10^{11})$W. This gives a ball-park figure of the power requirement of the geodynamo. More accurate estimates can be expected from specific geodynamo models. For example, Glatzmaier and Roberts estimate that at least 2×10^{11}W is required to balance ohmic diffusion (the dominant loss mechanism) in models of their type (Glatzmaier and Roberts 1995a,b, 1996a,b,c 1997). Recent estimates have put the total heat transfer from the core to the mantle at 8TW, with 6.8TW of that due to conduction in the core (Anderson 2002). Olson (2003) reviews the thermal interaction between the core and the mantle which has a vital controlling influence on the evolution of the whole of the Earth's deep interior.

The ohmic energy loss is made good by conversion [through the term $\boldsymbol{\nabla} \times (\mathbf{u} \times \mathbf{B})$ in (4a)] from the kinetic energy of the flow $\mathbf{u}$. In turn this kinetic energy must be continually replenished. There are two possible means of driving the flow: internal, by buoyancy forces and external, through forcing by boundary motion. The main candidates are: thermal convection (T), compositional convection (C), and precessionally driven flows (P). Cooling and radiogenic heating can lead to (T). The latent heat and light constituent release at the inner-core boundary (ICB) associated with the freezing of the inner core (see Section 1.2) can lead to (T) and (C). Precessional driving of core flows is due to the gravitational torques exerted on the Earth by the Sun and the Moon (see for example Malkus 1994).

Over the years, there has been considerable debate about the source of the core fluid motions driving the geodynamo. This has centered on two main issues: the power that can be extracted from a particular energy source, and the efficiency with which it can be converted into useful fluid motions (see for example Braginsky and Roberts 1995 for a detailed discussion). In the late 1970s, precession had been discounted on efficiency grounds and there were doubts as to the amount of radiogenic heating in the core and the efficiency of its conversion into kinetic energy, see for example Verhoogen (1980). This led to the revival of the idea of a *gravitationally-powered dynamo* whose energy source is the gravitational potential energy stored in the outer core. The gravitational potential energy is released as the Earth cools and the dense (almost pure iron) inner core grows by the freezing of iron from the outer core. Verhoogen (1961) was the first to associate freezing in the core with the dynamo power source. He discounted the chemical segregation associated with freezing of a mixture, preferring convection driven by the latent heat released during the crystallization of the inner core and the specific heat given out by the cooling core. Braginsky (1963) was the first to recognise the contribution of compositional effects. Their inherent efficiency together with the estimated power available made this an attractive power source when the other candidates appeared wanting on efficiency grounds.

Considerable progress has been made in understanding the complex process of freezing

of a mixture and applying the results to the Earth's core. Meanwhile, recent work on the other candidates means that precession should not be discounted (see for example Aldridge (2003)) and a question still remains about radiogenic heating (see for example Roberts *et al.* (2003)). For a more detailed discussion, see for example Fearn (1998).

The debate about what is driving the geodynamo continues and is linked with models for the thermal history of the Earth and the age of the inner core, see for example Labrosse *et al.* (2001), Roberts *et al.* (2003) and Gubbins *et al.* (2003, 2004). Most dynamo models still adopt thermally driven convection as the basis for their driving force, using a combination of internal and differential heating.

2 Governing equations and parameters

Our governing equations are the magnetic induction equation (**??**), the Navier-Stokes equations (**??**) (**??**) and the heat conduction equation (**??**). It is most convenient to deal with these in non-dimensional form. Adopting the outer-core radius r_o as our length scale, the ohmic diffusion time τ_η (1) as our time scale, r_o/τ_η as our velocity scale, $(\Omega\mu_0\rho_0\eta)^{1/2}$ (where $\Omega = 7.29 \times 10^{-5}\mathrm{s}^{-1}$ is the rotation frequency of the Earth and $\rho_0 = 1.1 \times 10^4\mathrm{kg\ m}^{-3}$ is the mean core density) as our scale for the magnetic field and βr_o (where β is a characteristic temperature gradient in the core) as the temperature scale, the governing equations become

$$\frac{\partial \mathbf{B}}{\partial t} = \boldsymbol{\nabla} \times (\mathbf{u} \times \mathbf{B}) + \Delta \mathbf{B}, \tag{4a}$$

$$\mathrm{E}_m \left(\frac{\partial \mathbf{u}}{\partial t} + (\mathbf{u} \cdot \boldsymbol{\nabla})\mathbf{u} \right) + 2\mathbf{k} \times \mathbf{u} = -\boldsymbol{\nabla} p + \mathrm{q}\widetilde{\mathrm{Ra}} T \mathbf{r} + \mathrm{E}\Delta \mathbf{u} + (\boldsymbol{\nabla} \times \mathbf{B}) \times \mathbf{B}, \tag{4b}$$

$$\boldsymbol{\nabla} \cdot \mathbf{u} = 0, \tag{4c}$$

$$\frac{\partial T}{\partial t} + \mathbf{u} \cdot \boldsymbol{\nabla} T = q\Delta T + \mathcal{E}, \tag{4d}$$

where $\mathcal{E}$ represents a source of heat. In most models, this is taken to be uniform. The effects of compressibility are not believed to be of primary importance in the dynamics of the core so the Boussinesq approximation is usually adopted. In this context, when applied to the core, the temperature T should be interpreted as the deviation from the adiabatic temperature. To include the effects of compressibility the anelastic approximation can be used, see (**??**). Glatzmaier & Roberts use this for all but the earliest of their models, see Section 5.3.

The non-dimensional parameters appearing in (4a)-(4d) are the modified Rayleigh number $\widetilde{\mathrm{Ra}}$, the magnetic Ekman number E_m, the Ekman number E and Roberts number q defined by

$$\widetilde{\mathrm{Ra}} = \frac{g_0 \alpha \beta r_o^2}{\Omega \kappa}, \quad \mathrm{E}_m = \frac{\eta}{\Omega r_o^2}, \quad \mathrm{E} = \frac{\nu}{\Omega r_o^2}, \quad \mathrm{q} = \frac{\kappa}{\eta}. \tag{5}$$

In the above we have written the gravitational acceleration as $g_0\mathbf{g}$ and taken $\mathbf{g} = -\mathbf{r}$, the non-dimensional position vector, since, to a fair approximation, the strength of the

gravitational acceleration increases linearly with radius in the core. The definition of $\widetilde{\mathrm{Ra}}$ is that most appropriate to a rotating magnetic system. The standard Rayleigh number, which is that normally used in non-rotating systems is

$$\mathrm{Ra} = \frac{g_0 \alpha \beta r_o^4}{\nu \kappa} = \frac{\widetilde{\mathrm{Ra}}}{\mathrm{E}}. \tag{6}$$

Here we shall usually simply refer to $(5)_1$ as the "Rayleigh number" and only use the term "modified Rayleigh number" when it is necessary to contrast it with (6).

The Ekman number E measures the strength of the viscous force (for length scales of the order of the core radius r_o) relative to the Coriolis force. The kinematic viscosity in the Earth's core is very poorly determined but most estimates are very much smaller than the magnetic diffusivity. A typical value for the Earth is $\nu \approx 10^{-6}$ m^{2}s^{-1} (de Wijs *et al.* 1998), giving $\mathrm{E} = O(10^{-15})$. It might therefore seem a very good approximation to neglect viscous effects altogether. In many fluid dynamical problems, provided the no-slip boundary conditions are also dropped, the *mainstream* flow (i.e. that away from narrow viscous boundary layers) is well approximated by an inviscid theory. (Then, the only role viscosity plays is to bring the tangential flow to zero at the boundaries. Such boundary layers are referred to as *passive*.) Unfortunately, in rotating systems, things are not so straightforward. The (Ekman) boundary layers are *active* or *controlling*; the mainstream solution cannot be completed without taking into consideration the flow in the Ekman layers, particularly the *Ekman pumping*, the flow out of the boundary layer into the mainstream. (Perhaps the simplest example of this is the flow between two parallel, differentially rotating plates, see, for example Chapter 8 of Acheson 1990.) So far, two complementary approaches have been adopted to deal with the problem of very small E. The first is to retain viscous terms and, for reasons of numerical resolution, we have to accept very much larger values of E than that given above. The alternative is to neglect viscous terms but have to accept the complications associated with Taylor's (1963) constraint (see Section 3.1). This is an example of the controlling influence of the boundary layers on the mainstream.

The magnetic Ekman number $(5)_2$ is sometimes referred to as the Rossby number. In the fluid dynamics literature, the Rossby number is defined as the ratio of the fluid speed to the rotational speed. The fluid speed will only emerge as part of the solution to (4a)-(4d) and the two definitions will only agree when the fluid speed is η/r_o. The magnetic Ekman number E_m is very much larger than E but is still small, $O(10^{-9})$, so the inertial terms in (4b) are often neglected; an approximation that filters out inertial waves and torsional oscillations (see Section 3.4) .

For the Earth's core, molecular diffusivity values give $\kappa \approx 8 \times 10^{-6}$ m^{2}s^{-1} (Poirier 2000), giving $q = O(10^{-5})$. Such a low value has important implications for the nature of convective flow, and for dynamo action. Current thought favours using $q = O(1)$ to avoid the various complications that arise when $q \ll 1$. This is the sensible approach until the complex interaction between flow and field that maintains the field is better understood. We discuss the choice of parameter values and the various restrictions on these in detail in Section 4.

There are two other important non-dimensional parameters that do not appear in (4a)-(4d). Had we chosen typical magnitudes $\mathcal{B}$ and $\mathcal{U}$ as our scales for the magnetic field and fluid velocity instead of those adopted above [$(\Omega\mu_0\rho_0\eta)^{1/2}$ and r_o/τ_η respectively], then $\mathbf{B}$ would be replaced by $\Lambda^{1/2}\mathbf{B}$ and $\mathbf{u}$ by $\mathrm{Rm}\,\mathbf{u}$, where the Elsasser number Λ and magnetic Reynolds number Rm are defined by

$$\Lambda = \frac{\mathcal{B}^2}{\Omega\mu_0\rho_0\eta}\ \left(= \frac{\sigma\mathcal{B}^2}{\Omega\rho_0}\ =\ \frac{\tau_\eta}{\tau_{MC}}\right), \qquad \mathrm{Rm} = \frac{\mathcal{U}r_o}{\eta}, \tag{7}$$

where the slow MHD time scale identified by Soward in Section **??** is given by

$$\tau_{MC} = \frac{\Omega}{{\Omega_A}^2}, \qquad \text{where} \quad {\Omega_A}^2 = \frac{\mathcal{B}^2}{\mu_0\rho_0 r_o^2}. \tag{8}$$

This is the time scale on which diffusionless magnetic waves evolve in a rapidly rotating system where $\Omega \gg \Omega_A$, the Alfvén frequency. For fully dynamic calculations, the scalings adopted here are the most appropriate since the amplitudes of $\mathbf{B}$ and $\mathbf{u}$ emerge as part of the solution. Hence Λ and Rm are not parameters that we can prescribe. In simpler model problems, though, the field and/or flow are often prescribed so that the alternative scalings based on $\mathcal{B}$ and $\mathcal{U}$ are often used. In either case, Λ and Rm are very useful non-dimensional measures of the field strength and flow speed respectively. Important alternative interpretations are in terms of the diffusivity η; both $\Lambda \to \infty$ and $\mathrm{Rm} \to \infty$ are associated with the perfectly conducting limit $\eta \to 0$.

For the Earth, a value of $\Lambda = 1$ roughly corresponds to a field strength of 1 mT, while $\mathrm{Rm} = 1$ corresponds to a flow speed of about 4×10^{-7} ms^{-1}. The latter, when compared with the flows inferred from the GSV suggest values of Rm of $O(10^3)$ when based on the core radius as length scale. This exceeds the lower bounds that have been derived for Rm if there is to be net field generation by dynamo action, see for example Moffatt (1978), Roberts (1994) and Chapter **??** and is consistent with the values found in hydrodynamic dynamo models (see Section 5).

3 Fundamental theoretical results

3.1 Taylor's Constraint

The smallness of the geophysical values of E and E_m suggests that both inertial and viscous terms be neglected in models of the core. This is the so-called *magnetostrophic approximation*. In this section we explore its fundamental consequences which clearly also have important implications for the behaviour of numerical solutions when E and E_m are small.

Setting $\mathrm{E}_m = 0$, $\mathrm{E} = 0$ in (4b) gives

$$2\mathbf{k} \times \mathbf{u} = -\boldsymbol{\nabla} p + \mathrm{q}\widetilde{\mathrm{Ra}}T\mathbf{r} + (\boldsymbol{\nabla} \times \mathbf{B}) \times \mathbf{B}. \tag{9}$$

Taking the ϕ-component gives

$$2u_s = -\frac{1}{s}\frac{\partial p}{\partial \phi} + [(\boldsymbol{\nabla} \times \mathbf{B}) \times \mathbf{B}]_\phi\,. \tag{10}$$

Integrating this over the cylinder $C(s)$, the cylinder of radius s coaxial with the rotation axis gives

$$2\int_{C(s)} u_s \, dS = \int_{C(s)} [(\boldsymbol{\nabla} \times \mathbf{B}) \times \mathbf{B}]_\phi \, dS \,, \quad \forall \, s \,. \tag{11}$$

The term on the left hand side is twice the net flow of fluid out of the curved surface of the cylinder.

If viscosity is totally neglected, (10) applies throughout the core and the cylinder extends to the boundaries of the outer core. There can therefore be no flow of fluid into or out of the ends of the cylinder. Consequently, for an incompressible fluid, the left hand side of (11) must vanish, giving

$$\int_{C(s)} [(\boldsymbol{\nabla} \times \mathbf{B}) \times \mathbf{B}]_\phi \; dS \;=\; 0, \qquad \forall \; s. \tag{12}$$

This condition was first derived by Taylor (1963) and is referred to as "Taylor's condition" or "Taylor's constraint". It can be interpreted as that the net magnetic torque on each cylinder must vanish.

If viscous effects are retained in the problem, (but are only important in thin Ekman layers at the boundaries of the outer core) then (10) is valid throughout the core except for the Ekman layers, and the cylinder $C(s)$ must be considered as extending, not to the boundaries of the outer core, but to the outer edges of the Ekman layers. The North-South flow in the Ekman layers leads to a net flow of fluid into the ends of the cylinder. This must be balanced by a net flow out of the curved surface of the cylinder, so the left hand side of (11) is in general non-zero. To evaluate $\int_{C(s)} u_s \, dS$ we must calculate the flow in the Ekman layers.

The problem is analysed by splitting the core into three regions, a thin spherical shell that extends inward a short distance from the core-mantle boundary, a similar shell adjacent to the boundary with the inner core, and the *interior*, which is the remainder (and the bulk of) the outer core. In the interior, viscous effects are negligible, and (10) holds. In the two boundary regions, viscous effects are important. The short length scale in the radial direction permits a simplification to the governing equations and an analytical solution. This must then be matched to the solution in the interior. The spherical geometry is unimportant in the boundary layers and can locally be approximated by a plane layer. In general, we define, for any $f = f(r, \theta, \phi)$ its azimuthal mean

$$\overline{f}(r, \theta) \;\equiv\; \overline{f} \;\equiv\; \frac{1}{2\pi} \int_0^{2\pi} f \, d\phi. \tag{13}$$

The analysis relates the mean azimuthal flow $\overline{u}_\phi$ at the edge of the boundary layer to the flow in the boundary layer in the θ-direction. The latter is related to the left hand side of (11) since, for an incompressible fluid, the flow into the top and bottom of the cylinder $C(s)$ must be matched by a flow out through its curved surface. The boundary-layer analysis then allows us to relate $\overline{u}_\phi$ to the right hand side of (11). Details can be found, for example in Fearn (1994) [but note that he uses an alternative definition of E that differs

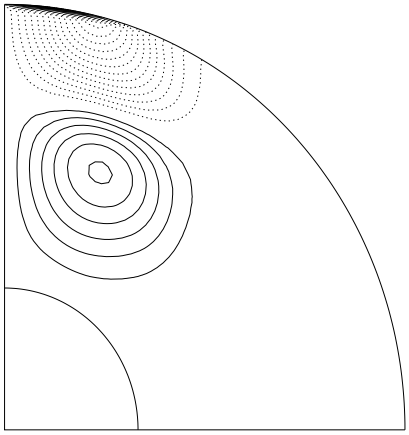

Figure 4: An example of a solution satisfying Taylor's constraint. Shown are contour plots of $\overline{[(\boldsymbol{\nabla}\times\mathbf{B})\times\mathbf{B}]}_\phi$. Contour interval is 1. Solid lines represent positive and dashed lines represent negative contours.

[1]

by a factor 2 and the factor 2 then does not appear in the Coriolis force term in (9)]. The boundary-layer analysis can be found in Section 4.4 of Batchelor (1967). We find, for the case where s is outside the tangent cylinder ($s > r_i$), and $\overline{u}_\phi(s, z_T)$ is assumed to take the same value as $\overline{u}_\phi(s, z_B)$ that

$$\overline{u}_\phi(s, z_T) \;=\; \frac{1}{2}\left(\frac{\cos\theta}{\mathrm{E}}\right)^{\frac{1}{2}} \mathcal{T}\,, \tag{14}$$

where

$$\mathcal{T}(s) = \int_{z_B}^{z_T} \overline{[(\boldsymbol{\nabla}\times\mathbf{B})\times\mathbf{B}]}_\phi \; dz\,, \tag{15}$$

and $z_T = \sqrt{1-s^2}$ and $z_B = -z_T$. This replaces (12) when the effects of Ekman boundary layers are included in the problem.

We note here that (12) and (14) are very different in character. The former is a constraint on $\mathbf{B}$ while the latter is a means of determining $\overline{u}_\phi$. In a typical small E solution we shall expect $\mathcal{T}$ also to be small. For $O(1)$ values of $|\mathbf{B}|$ this is achieved by regions of positive $\mathcal{T}$ cancelling with regions of negative $\mathcal{T}$ in the integral, see Figure 4. The balance is delicate and can be expected to be difficult numerically.

3.2 The "arbitrary" geostrophic flow $u_G(s)$

If (12) is satisfied then we can solve (9) for $\mathbf{u}$, given $\mathbf{B}$ and T, as we see below. However, the solution is not unique. If we add any $u_G(s)\mathbf{e}_\phi$ to $\mathbf{u}$, then the additional Coriolis term can be written as

$$\mathbf{k}\times u_G(s)\mathbf{e}_\phi = -u_G(s)\mathbf{e}_s = -\boldsymbol{\nabla}\left(\int u_G(s)\,ds\right)\,, \tag{16}$$

and hence can be absorbed into the pressure gradient term. Consequently if $\mathbf{u}$ is a solution of (9), then so is $\mathbf{u} + u_G(s)\mathbf{e}_\phi$ for arbitrary $u_G(s)$.

Taking the curl of (9), and using (4c) gives

$$-2\frac{\partial \mathbf{u}}{\partial z} = \boldsymbol{\nabla} \times [(\boldsymbol{\nabla} \times \mathbf{B}) \times \mathbf{B}] + \mathrm{q}\widetilde{\mathrm{Ra}}(\boldsymbol{\nabla} T \times \mathbf{r}). \tag{17}$$

Taking the axisymmetric part and integrating this with respect to z gives

$$2\overline{\mathbf{u}} = \int_z^{z_T} \overline{\boldsymbol{\nabla} \times [(\boldsymbol{\nabla} \times \mathbf{B}) \times \mathbf{B}]}\, dz' \;+\; \mathrm{q}\widetilde{\mathrm{Ra}} \int_z^{z_T} \overline{(\boldsymbol{\nabla} T \times \mathbf{r})}\, dz' \;+\; \mathbf{F}(s), \tag{18}$$

where $\mathbf{F}(s)$ is an arbitrary function of integration. The flow $\overline{\mathbf{u}}$ must satisfy the boundary condition that (to leading order) there is no normal flow at the top and bottom boundaries. These two boundary conditions give two expressions relating $\overline{u}_s$ and $\overline{u}_z$ which then determine F_s and F_z. In a non-axisymmetric system, the third component $\overline{u}_\phi$ of the flow would be determined from $\boldsymbol{\nabla} \cdot \mathbf{u} = 0$. However, in this axisymmetric system $\overline{u}_\phi$ is independent of ϕ and so does not appear in $\boldsymbol{\nabla} \cdot \mathbf{u}$. Consequently F_ϕ is undetermined and we call it the *"arbitrary" geostrophic flow* u_G. We then have

$$\overline{u}_\phi \;=\; u_M \;+\; u_T \;+\; u_G\,, \tag{19}$$

where

$$u_M \;=\; \frac{1}{2}\int_z^{z_T} \overline{\boldsymbol{\nabla} \times [(\boldsymbol{\nabla} \times \mathbf{B}) \times \mathbf{B}]}_\phi\, dz' \tag{20}$$

is the *magnetic wind*, and

$$u_T \;=\; \frac{1}{2}\mathrm{q}\widetilde{\mathrm{Ra}} \int_z^{z_T} \overline{(\boldsymbol{\nabla} T \times \mathbf{r})}_\phi dz' \tag{21}$$

is the *thermal wind* familiar in the meteorological literature (see for example Roberts & Soward, 1978). Note that with our choice of the limits of integration in (20)-(21), $u_M = u_T = 0$ at $z = z_T$. Consequently the geostrophic flow $u_G = \overline{u}_\phi|_{z_T}$.

The apparent arbitrariness of the geostrophic flow u_G is a consequence of considering (9) in isolation; of considering the forcing terms on the right hand side as prescribed, rather than as determined through (4a) and (4d). In practice u_G is not arbitrary. The manner in which it is determined depends on the importance of the Ekman suction.

3.3 Ekman states, Taylor states and model-Z: determination of the geostrophic flow u_G

If Taylor's condition (12) is satisfied, then (9) can be solved for $\mathbf{u}$ up to the unknown geostrophic flow. As Fearn & Proctor (1992) point out, it is the very existence of a "homogeneous solution" of the form $u_G(s)\mathbf{e}_\phi$ that makes a "solvability condition" of the form (12) necessary. Of course, $u_G(s)$ can only be considered as arbitrary in the context of

solving (9) for a given right hand side when (12) is satisfied. In practice, u_G is determined in one of two ways. Either Ekman suction is important, so the left hand side of (11) is non-zero and Taylor's condition does not apply. Then we know $\overline{u}_\phi$ at the boundary through an expression like (14). This extra piece of information determines u_G explicitly. Alternatively, Taylor's condition does apply. The system (4a-4d) then must adjust the magnetic field so that Taylor's condition is satisfied. The mechanism used to achieve this is to adjust the differential rotation (the ω-effect discussed in Chapter **??**) by varying u_G. The differential rotation stretches out poloidal field to generate toroidal field. By varying u_G, B_ϕ can be adjusted and perhaps (12) satisfied. This mechanism determines u_G in a very complicated implicit manner.

There is no guarantee that (12) can be satisfied. Fearn & Proctor (1987) tackled the problem of the determination of u_G through this mechanism, by choosing u_G to minimise the absolute value of the left hand side of (12) for a given poloidal magnetic field and a flow that is prescribed (apart from the geostrophic flow). Their method was very successful for certain choices of field and flow, but gave poor results for other choices.

Non-axisymmetric magnetoconvection models and kinematic α^2- and $\alpha\omega$-dynamo models and have been adapted to include a geostrophic flow determined by an expression similar to (14). Without the feedback due to the geostrophic flow, both problems are linear and would show exponential growth of their solutions for a sufficiently large forcing. For forcing just above critical, the systems typically find themselves in an "Ekman state" where equilibration of the amplitude of the solution is achieved through the action of the geostrophic flow. In this respect, it is the condition (14) that provides the dominant nonlinear effect, since it becomes important at much smaller amplitude of solution than all other nonlinear effects. The reason for this is the small value of the Ekman number, giving an equilibrated solution amplitude of $O(\mathrm{E}^{\frac{1}{4}})$ (see Section 7.3 of Fearn, 1994). As the driving force is increased, the system usually evolves to a state where (12) is satisfied (a "Taylor state") and it is the other nonlinear effects that are responsible for equilibration, this time at higher [$O(1)$] amplitude; viscous effects no longer have a major influence on the solution.

This picture of the nonlinear evolution of a dynamo has come to be known as the Malkus-Proctor scenario, see Malkus & Proctor (1975). It is not the only possible manner in which a dynamo can evolve. An (or the) alternative is where the Taylor state is replaced by a state in which the solution amplitude is $O(1)$ but where viscous effects remain important, even in the limit $\mathrm{E} \to 0$. This is Braginsky's (1975) model-Z (see also Braginsky, 1994). Its fundamental difference from a Taylor state is the manner in which Taylor's constraint is satisfied or almost satisfied. In a Taylor state, with $|\mathbf{B}|$ of $O(1)$, (12) is satisfied with $\mathcal{T}$ [see (15)] of $O(1)$ everywhere and regions of positive $\mathcal{T}$ cancelling with regions of negative $\mathcal{T}$ when the integral over $C(s)$ is taken. (This cancellation effect is illustrated well in Fearn & Proctor, 1987.) There is strong coupling between adjacent cylinders [since $\mathcal{T}$ is $O(1)$], providing the mechanism for Taylor's condition (12) to be maintained as the system evolves. By contrast, in model-Z, (12) is almost satisfied, by $\mathcal{T}$ being small everywhere. This is achieved by having B_s close to zero, while B_ϕ, B_z are $O(1)$. This is because an alternative expression of Taylor's constraint (for an axisymmetric field and an insulating

mantle) is

$$\int_{z_B}^{z_T} B_\phi B_s \, dz = 0, \tag{22}$$

see for example Fearn (1994). The meridional field is then almost aligned with the z-axis, hence the name of the model. Since B_s is small, there is only small coupling between adjacent cylinders $C(s)$ and the system is unable to satisfy Taylor's condition exactly. Consequently, the geostrophic flow remains dependent on the strength of core-mantle coupling. Here, we have concentrated on viscous core-mantle coupling, so u_G remains dependent on E, and very large geostrophic flows are found in the limit of small E, see for example Braginsky & Roberts (1987).

Note that in the above discussion we have used the description "$O(1)$" rather loosely. This has been to avoid too detailed a discussion of the appropriate scalings and to focus on the important distinction between the small amplitude Ekman state and the high amplitude Taylor and model-Z states. Model-Z is discussed in detail in Braginsky (1994), and the relationship between model-Z and Taylor states in Roberts (1989). The nonlinear role of the geostrophic flow on kinematic dynamo and magnetoconvection models is discussed in detail in Fearn (1994).

3.4 The role of inertia

An arbitrary initial condition will not necessarily satisfy Taylor's constraint, in which case (9) has no solution. Of course, the full equation (4b) can quite happily be time-stepped for arbitrary initial conditions. Taylor (1963) comments that if his constraint is not satisfied then "rapid torsional motion would be set up in which each concentric cylindrical annulus rotated as a rigid body. The adjacent annuli are coupled together, as if by elastic strings, through the magnetic field B_s. Because of this linkage, the torsional motion would modify the fields until a state was reached in which (12) was satisfied". Taylor (1963) envisaged that, in a short time, this adjustment would take place. Subsequently, the flow would continue to adjust in just the manner required to ensure that Taylor's constraint continued to be satisfied. Indeed this is the process that determines the geostrophic flow u_G in a Taylor state.

Should Taylor's constraint fail to be satisfied, the azimuthal torque (15) on cylinders will be non-zero and the $\mathrm{E}^{-\frac{1}{2}}$ factor in (14) indicates the generation of a strong geostrophic flow. Inertia must then inevitably play a role. If we retain inertia in our problem, but only for a geostrophic flow $u_G(s)\mathbf{e}_\phi$, we can repeat the analysis of Section 3.1 to obtain, in place of (14),

$$2z_T \mathrm{E}_m \frac{\partial u_G}{\partial t} + 2\left(\frac{\mathrm{E}}{\cos\theta}\right)^{\frac{1}{2}} u_G \;=\; \mathcal{T}\,. \tag{23}$$

The addition of the inertial term can be of assistance in finding steady solutions, playing a technical role, preventing numerical instabilities in the small E limit, see Jault (1995), in particular his equation (6). Glatzmaier & Roberts (1996a) introduced the axisymmetric

azimuthal part of inertia into their 3D hydrodynamic dynamo model, having neglected inertia in their earlier work (Glatzmaier & Roberts 1995a,b).

In the limit of small E, (23) becomes an equation for *torsional oscillations*

$$2z_T \mathrm{E}_m \frac{\partial u_G}{\partial t} \;=\; \mathcal{T}\,. \tag{24}$$

An additional equation can be obtained by taking the expression (15) and differentiating it with respect to t:

$$2\pi s \frac{\partial \mathcal{T}(s,t)}{\partial t} \;=\; \int_{C(s)} \left[(\boldsymbol{\nabla}\times\mathbf{B})\times\frac{\partial \mathbf{B}}{\partial t}\right]_\phi + \left[(\boldsymbol{\nabla}\times\frac{\partial \mathbf{B}}{\partial t})\times\mathbf{B}\right]_\phi dS\,. \tag{25}$$

Substituting for $\partial\mathbf{B}/\partial t$ from the induction equation (4a) and neglecting the diffusion term, for an axisymmetric field it can be shown that

$$2\pi s \frac{\partial \mathcal{T}(s,t)}{\partial t} \;=\; a(s)\frac{\partial^2}{\partial s^2}\left(\frac{u_G}{s}\right) + b(s)\frac{\partial}{\partial s}\left(\frac{u_G}{s}\right) + c(s) \tag{26}$$

where

$$a(s) = \int_{C(s)} s B_s^2\, dS\,, \qquad b(s) = \int_{C(s)} \left(s\,\mathbf{B}\cdot\boldsymbol{\nabla}B_s + 2B_s^2\right)\, dS\,, \tag{27}$$

and $c(s)$ contains all the other contributions that do not involve u_G. Note that Taylor(1963) derived a version of this equation, without the left-hand-side by differentiating (12) rather than (15). It was Braginsky (1970) who first derived an equation describing torsional waves.

Equations (24) and (26) form a hyperbolic system which may be expected to admit oscillatory solutions about the steady state for which $\mathcal{T} = 0$ (Moffatt, 1978). In these torsional oscillations, each cylinder $C(s)$ rotates about its axis. Recall that flows of the form $u_G(s)\mathbf{e}_\phi$ are unaffected by the Coriolis force, see (16). The oscillations are controlled by their magnetic linkage through B_s and the shearing of this field component by differential rotation; notice that it is only radial gradients of u_G/s that appear in (26). The time scale of the torsional oscillations can be determined by combining (24) and (26). We find that

$$\mathrm{E}_m \frac{\partial^2}{\partial t^2} \;\sim\; B_s^2\,. \tag{28}$$

Recalling that time has been non-dimensionalised using τ_η and $\mathbf{B}$ using $(\Omega\mu_0\rho_0\eta)^{\frac{1}{2}}$ we conclude that the characteristic time for torsional waves is

$$\frac{{\mathrm{E}_m}^{\frac{1}{2}}}{B_s}\tau_\eta \;=\; \frac{1}{B_s}\left(\tau_\eta\Omega^{-1}\right)^{\frac{1}{2}} \;=\; r_o\frac{\sqrt{\mu_0\rho_0}}{B_s^*}\,, \tag{29}$$

where B_s^* is the dimensional radial field. From this we can see that the time scale of torsional waves is essentially determined by the time it takes an Alfvén wave propagating on the radial field to travel a distance of the order of the radius of the core. If we choose

an average radial field strength of 0.1mT then the above gives a time of the order of 130 years. Stronger fields give shorter times. Section 3 of Roberts & Soward (1972) gives a more detailed analysis including a discussion of the decay of torsional oscillations.

Braginsky (1970) invoked torsional oscillations as a possible mechanism for explaining observations of variations in the length of the day with a period of about 60 years (he assumed a field strength of 0.186mT). Jault & Le Mouël (1991) also investigated the problem, looking in detail at electromagnetic and topographic core-mantle coupling. Torsional oscillations continue to be of interest as mechanism for explaining observations. For example Pais & Hulot (2000) see evidence for torsional oscillations in their analysis of core flow at the CMB deduced from geomagnetic models, and Bloxham *et al.* (2002) in an analysis of geomagnetic data show that "geomagnetic jerks can be explained by the combination of a steady flow and a simple time-varying, axisymmetric, equatorially symmetric, toroidal zonal flow. Such a flow is consistent with torsional oscillations in the Earths core". Jault (2003) reviews this area.

4 Parameter Constraints

The choice of the values for freely prescribable parameters in geodynamo models is a compromise between realistic values for planetary interiors and computationally tractable values. The balance will move to the former as our understanding of the problem, computational techniques and computational power advance, but initially a practical approach is wise; adopting values that produce well-resolved solutions. Here we summarise some results from model problems that illustrate the dependence of solutions on key parameters and discuss how these constrain what values of these parameters we can reasonably use in geodynamo models.

4.1 The Ekman number

As discussed in Section 2, using typical estimates of the molecular viscosity, and the radius of the Earth's outer core as our length scale, the Ekman number $\mathrm{E} = O(10^{-15})$. It is this very small value that is the most fundamental source of difficulty in solving the geodynamo problem. The (Ekman) boundary layers at the CMB and ICB each have thickness of $O(\mathrm{E}^{\frac{1}{2}})$ (equivalent to about 0.1m for the Earth). In a non-magnetic system (where the leading order balance is geostrophic) both the convective length scale (see Section **??**) and the shortest length scale of the Stewartson-layer structure (see Section **??**) associated with the tangent cylinder are of $O(\mathrm{E}^{\frac{1}{3}})$. Clearly, resolution of such structures in any numerical scheme is impossible for any realistic value of E. The Stewartson-layer structure is modified by the presence of a magnetic field (see Soward & Hollerbach 2000) but any simulation has to be able to deal with situations where the field is, at least locally, weak. The stiffness associated with Taylor's constraint in the limit of small E (see Section 3.1) is a further difficulty. The only options are to work with much larger values of E or to adopt the magnetostrophic approximation $\mathrm{E} = 0$. Work by Walker *et al.* (1998) has identified a

problem that affects both the $\mathrm{E} = 0$ and $\mathrm{E} \to 0$ cases; the development of small scale, high frequency waves, implying a time step of order $\mathrm{E}\tau_\eta$ to ensure numerical stability. This has proved an insurmountable problem in attempts to work in the magnetostrophic approximation.

Significant progress has been made using the finite E approach (see Section 5). Even with substantial supercomputer resources, it is not feasible to reduce E much below 10^{-5} (see for example Jones *et al.* 1995, Kuang & Bloxham 1997, 1999). To lower, what we might call the *headline Ekman number*, some authors have adopted so-called *hyperdiffusivities*. These enhance the diffusivity for short length scales in the θ- and ϕ-directions. Solutions are typically expressed through expansions in spherical harmonics, for example

$$g = \sum_{l=m}^{L} \sum_{m=0}^{M} g_{lm}(r) P_l^m(\cos\theta) \mathrm{e}^{\mathrm{i}m\phi} \; + \; c.c., \tag{30}$$

where g is the toroidal part of the field, P_l^m are associated Legendre functions (see for example Abramowitz and Stegun 1965) and *c.c.* denotes complex conjugate. Then, an example of hyperdiffusivity is defined by

$$\nu = \overline{\nu}(1 + hl^3), \tag{31}$$

where h is some constant and l is the spherical harmonic degree. It is then $\overline{\nu}$ that appears in the definition of the Ekman number rather than ν. The effect of the hyperdiffusivity is to "damp small scales while allowing the large scales to experience much less diffusion" (Glatzmaier and Roberts 1995b). Glatzmaier and Roberts (1995b) use $h = 0.075$, achieving a headline Ekman number of 2×10^{-6}. The other diffusivities κ and η are treated in the same manner. More recently, Glatzmaier and Roberts have used $h = 0.037$ for ν and κ and 0.016 for η (Glatzmaier and Roberts 1996b,c). The argument typically put forward to justify the use of hyperdiffusivities is that the diffusivities are assumed to be eddy (subgrid) diffusivities and the small resolved eddies physically interact more strongly with the small unresolved eddies so they should have larger diffusivities. The use of hyperdiffusion does distort the dynamics of the core, resulting in viscosity retaining a controlling influence on the geostrophic flow, for example, see Zhang & Jones (1997).

An important issue that is relevant to the question of how low E must be in order to be characteristic of the geodynamo is highlighted by Jones (2000). He discusses whether the geodynamo is supercritical or subcritical, in the following sense. It is well known from linear studies (see for example Proctor 1994) that, in a rapidly rotating system, the modified Rayleigh number for the onset of thermally driven convection $\widetilde{\mathrm{Ra}}_{c0} \equiv \widetilde{\mathrm{Ra}}_c(\mathbf{B} = \mathbf{0})$ is of $O(\mathrm{E}^{-\frac{1}{3}})$ in the absence of any magnetic field. By contrast, in the presence of a prescribed magnetic field with $\Lambda = O(1)$, $\widetilde{\mathrm{Ra}}_c$ reduces to $O(1)$; the presence of the field facilitates convection. Numerical studies (see Section 5.3) show that $\widetilde{\mathrm{Ra}}$ may have to be well above its critical value in order to maintain a field. Nonetheless, when $\mathrm{E} \ll 1$, it is possible that a self-sustaining dynamo exists for $\widetilde{\mathrm{Ra}} < \widetilde{\mathrm{Ra}}_{c0}$. Jones (2000) calls this situation a *subcritical dynamo* and estimates that dynamos for $\mathrm{E} < 10^{-10}$ must be subcritical. They

may exist at larger values of E but all numerical models so far have required $\widetilde{\mathrm{Ra}} > \widetilde{\mathrm{Ra}}_{c0}$ for dynamo action, see for example Busse *et al.* (2003). Gubbins (2001) argues that the Rayleigh number in the core is highly supercritical.

4.2 The magnetic Reynolds number

The magnetic Reynolds number Rm is a non-dimensional measure of the relative importance of the induction term $\boldsymbol{\nabla} \times (\mathbf{u} \times \mathbf{B})$ to the diffusive term $\Delta \mathbf{B}$. In the absence of the former, it can be shown that the field $\mathbf{B}$ inevitably decays. For field maintenance, the induction effect must be able to at least balance the diffusive losses; i.e. Rm must exceed some minimum value [$\geq O(1)$]. Specific lower bounds on Rm for dynamo action can be derived, see for example Roberts (1994) and Chapter **??**.

In a fully hydrodynamic dynamo model, the flow $\mathbf{u}$ emerges as part of the solution so Rm is not a parameter that can be freely chosen. The vigour of the flow depends on the forcing whose magnitude is determined by the modified Rayleigh number $\widetilde{\mathrm{Ra}}$ (see below). The level of the forcing must be sufficient that dynamo action is taking place, while at the same time ensuring that Rm (which measures the strength of the differential rotation) is not too large. Shear acts to inhibit convection (see for example Fearn & Proctor, 1983) and associated with this are short length scales typically $O(\mathrm{Rm}^{-\frac{1}{3}})$. If Rm is too large, such length scales may be difficult to resolve.

4.3 The Roberts number

The situation described above is worse when the Roberts number q is small. Differential rotation begins to have a significant effect when $\mathrm{Rm} = O(\mathrm{q})$ with length scales $O(\mathrm{Rm}/\mathrm{q})^{-\frac{1}{3}}$ having to be resolved. With the requirement for dynamo action that Rm be at least $O(1)$ there is a clear problem when q is small, as is appropriate if we use molecular values of the diffusivities. The situation may be helped somewhat in that strong fields act to oppose shear (see for example Busse 2002). Small values of q have also been problematical in attaining solutions satisfying Taylor's constraint (see Section 3.1 and Soward 1986, Skinner & Soward 1988, 1990). Further, peculiar features are present in the $\widetilde{\mathrm{Ra}}$ versus Λ graph for the onset of thermally driven convection when $q \ll 1$ (see Zhang & Jones 1996).

The source of many of these problems is the mismatch between the thermal and ohmic time scales [$\tau_\kappa = r_o^2/\kappa$ and τ_η, see (1)]. With molecular values of the diffusivities, $\tau_\eta = O(10^5)$ years. This is an upper bound on the time scale on which the dynamo must regenerate magnetic field. With $\mathrm{q} = O(10^{-5})$ (see Section 2), the natural thermal time scale is longer than the age of the Earth. This mismatch is probably also the source of the much higher values of $\widetilde{\mathrm{Ra}}$ found to be required for dynamo action when q is small, see for example the discussion in Jones (2000), Busse (2002, Figure 15) and below.

It is clear that, initially, to make progress, it is sensible to adopt $O(1)$ values of q. Indeed, parameter surveys have shown no dynamo action for q less than some critical value q_c which decreases with decreasing E, see for example Christensen *et al.* (1999).

They choose Pr = 1 so q = Pm. They found dynamo action only for $\mathrm{Pm} > \mathrm{Pm}_c \sim 450\mathrm{E}^{\frac{3}{4}}$. For $\mathrm{E} = 10^{-3}$, $\mathrm{Pm}_c \sim 2$ and for $\mathrm{E} = 10^{-4}$ they found $\mathrm{Pm}_c \sim 0.5$.

4.4 The Rayleigh number

The above discussion about disparate time scales suggests that very highly supercritical values of $\widetilde{\mathrm{Ra}}$ will be required for dynamo action if q is small. This is consistent with the findings of Glatzmaier and Roberts (1995a,b) who use q = 0.1. Jones *et al.* (1995) find dynamo action at much smaller values of $\widetilde{\mathrm{Ra}} - \widetilde{\mathrm{Ra}}_{c0}$ for q = 10 compared with q = 1. The form of the buoyancy term in (4b) suggests that it is $\mathrm{q}\widetilde{\mathrm{Ra}}$ that is important for dynamo action.

4.5 The magnetic Ekman number

Motivated by the smallness of E_m, some numerical models of the geodynamo neglect inertial terms altogether, a few choose the geophysical value, while many take the view that E_m should be no smaller than the Ekman number. The magnetic Prandtl number

$$\mathrm{Pm} = \mathrm{E}/\mathrm{E}_m = \nu/\eta \tag{32}$$

is small in the core but the numerical constraints on E mean that most numerical models take $\mathrm{Pm} = O(1)$. Taking the geophysical value of E_m while accepting the numerical constraints on E would imply a large magnetic Prandtl number, while neglecting inertial effects altogether corresponds to the infinite magnetic Prandtl number limit. Whatever the choice, almost all studies choose a fixed value of E_m and focus on other aspects of the problem. Very little work has focussed in on the role of inertia in the dynamo problem (but see Fearn & Morrison, 2001; Fearn & Rahman 2004b). Fearn & Morrison (2001) find that dynamo action shuts off as E_m is increased. This is consistent with the studies (see Section 4.3) that show no dynamo action if q or equivalently Pm is too small.

5 Numerical models

There has been considerable progress over the past 10 years in modelling the geodynamo, with many groups now actively involved. Reviews include those by Dormy *et al.* (2000), Jones (2000), Roberts & Glatzmaier (2000), Busse (2002), Glatzmaier (2002) and Kono & Roberts (2002). In making comparisons between different calculations, care should be taken to note that different authors use different definitions of the key non-dimensional parameters. The two main differences are:

- whether the factor 2 is retained, as here [see (4b)], in the Coriolis force or whether it is absorbed into the definitions of E, $\widetilde{\mathrm{Ra}}$, E_m and Λ,
- the choice of length scale. Here we have used the outer core radius r_o. Many papers use the core gap width $r_o - r_i$, and of course there are variations on the choice of r_i.

In the following discussion, where we give values of dimensionless parameters, we are simply quoting the values given by the authors; we have not attempted to normalise them to the definitions used here.

5.1 Nonlinear α^2 and $\alpha\omega$ models

Proctor, in Chapter **??**, has described linear mean-field α^2- and $\alpha\omega$-dynamos. For these, in the supercritical regime, a seed field will grow without bound. In the context of the geodynamo, the first nonlinear effect that becomes important as $\mathbf{B}$ grows in strength is the geostrophic flow discussed in Section 3.1. The $\mathrm{E}^{-\frac{1}{2}}$ factor in (14) implies u_G is of $O(1)$ when $|\mathbf{B}|$ is of $O(\mathrm{E}^{\frac{1}{4}})$. The system is then in an Ekman state. A number of studies have investigated the role of the geostrophic flow in equilibrating mean-field dynamos. As the driving is increased (an increase in the strength of α and/or ω), the system typically evolves towards a state in which Taylor's constraint (12) is satisfied as envisaged by Malkus & Proctor (1975), though the manner in which this happens is model dependent, see for example Soward & Jones (1983). If the only nonlinear effect that is included in a model is u_G, then, when (12) is satisfied, the solution is no longer viscously controlled and will grow without bound. Other (ageostrophic) nonlinear effects then must come into play to equilibrate the solution with $|\mathbf{B}| = O(1)$ in a Taylor state. Studies using a spherical geometry include those by Proctor (1977), Hollerbach & Ierley (1991), Barenghi (1992) and Hollerbach & Jones (1993, 1995). The latter solved

$$\frac{\partial \mathbf{B}}{\partial t} = \boldsymbol{\nabla} \times (\mathbf{u} \times \mathbf{B} + \alpha \mathbf{B}) + \Delta \mathbf{B}, \tag{33a}$$

$$2\mathbf{k} \times \mathbf{u} = -\boldsymbol{\nabla} p + \Theta \mathbf{r} + \mathrm{E} \Delta \mathbf{u} + (\boldsymbol{\nabla} \times \mathbf{B}) \times \mathbf{B}, \tag{33b}$$

together with (4c) for axisymmetric $\mathbf{B}$ and $\mathbf{u}$ and prescribed α and Θ. The term $\Theta\mathbf{r}$ models the buoyancy force, driving a meridional circulation as well as differential rotation.

This system retains the simplicity of the mean-field dynamo by parameterising non-axisymmetric effects by the α-effect while including the key nonlinear interactions between $\mathbf{B}$ and $\mathbf{u}$; the field drives a flow through the action of the Lorentz force in (33b) and this flow acts back on the field in (33a).

Hollerbach & Jones (1993, 1995) considered a system with a finitely conducting inner core and demonstrated the stabilising effect it could have on dynamo solutions. Fotheringham *et al.* (2002) and Fearn & Rahman (2004a) have extended the model to investigate the stability of axisymmetric fields to non-axisymmetric instabilities and found that such instabilities can significantly constrain the strength of field that can be generated.

5.2 2.5D models

The term "2.5D" is applied to models that solve the convectively-driven system (4a)-(4d), resolving fully in radius r and colatitude θ but with only very restricted resolution in azimuth ϕ. The motivation for this is to produce a problem that is tractable with

moderate computing resources. The justification is from Cowling's theorem (see Chapter **??**). We know that an axisymmetric field cannot be maintained by fluid motions. The interaction between axisymmetric and non-axisymmetric parts of the system are therefore a key ingredient of the dynamo problem. So, simply considering the axisymmetric part and even one non-axisymmetric mode ensures that this key ingredient is present in the model.

Jones *et al.* (1995) reported the first results from a 2.5D model. The results were encouraging, producing fields of around the right magnitude and associated with flow strengths consistent with those deduced from the secular variation. Most of their calculations are for an Ekman number of 10^{-3} (note that their definitions of the Ekman and modified Rayleigh numbers have a factor 2 in the denominator and are based on the gap-width $r_o - r_i$ as length scale). Their single non-axisymmetric mode has azimuthal wavenumber $m = 2$. They consider both q = 10 and q = 1 and find that while for $\widetilde{\mathrm{Ra}}_J = 50$ (a subscript J denotes their definition of the parameter) is sufficient to maintain a dynamo for q = 10, $\widetilde{\mathrm{Ra}}_J = 1600$ was required to sustain a field when q = 1. This feature of increasing $\widetilde{\mathrm{Ra}}$ with decreasing q is one that is reinforced by 3D studies.

Subsequent studies have proceeded to use the model to investigate, for example, the effect of varying the Ekman number (Sarson & Jones 1998), the effect of CMB heterogeneity (Sarson *et al.* 1997) and reversals (Sarson & Jones 1999, Sarson 2000). The model has been used to good effect in elucidating the results from 3D models and in understanding dynamo behaviour in different parameter regimes (see below and Jones 2000).

5.3 3D models

The first attempts at 3D calculations were by Zhang & Busse (1989, 1990). Their calculations used stress-free boundary conditions which reduces the problem of resolving viscous boundary layers. This was appropriate since computing resources were limited; allowing only modest space resolution. Furthermore, resolution in time was restricted to a single mode; they did not use a time-stepping method, instead following a bifurcation sequence from stationary fluid, to steadily drifting finite amplitude convection, to a finite amplitude convection driven dynamo. Solutions were sought proportional to $\exp[\mathrm{i}(\phi - ct)]$ so all components of the solution were forced to drift at the same wave speed c. They used $\mathrm{E} = 10^{-3}$ and found dynamo solutions. Unfortunately, attempts to follow these to lower E failed; the dynamo action found did not persist as E was reduced.

The fully 3D time-stepping calculation of Glatzmaier & Roberts (1995a,b) marked a major step forward. They used q = 0.1 and found maintenance of a field of strength up to 56 mT. Glatzmaier & Roberts found that very high values of their Rayleigh number ($g\alpha Q/2\Omega c_p \rho \kappa^2 \approx 6 \times 10^7$, where Q is the heat flux at the bottom of the core and c_p the specific heat capacity) were required to give dynamo action. This high value at small q is consistent with the trend found by Jones *et al.* (1995) who speculate that the reason is that convective velocities scale with $\mathrm{q}\widetilde{\mathrm{Ra}}$ rather than $\widetilde{\mathrm{Ra}}$. The single integration of Glatzmaier & Roberts (1995a,b) required substantial supercomputer resources and simulated only 40,000

years. An important feature of the simulation was that it included a field reversal.

Following on from this pioneering work, several groups have produced their own geodynamo models. Increasing computing power has allowed longer integrations and modest exploration of parameter space. Most models use a similar (spectral) numerical approach (see for example Hollerbach 2000) and give good agreement for a simple steady benchmark solution (see Christensen *et al.* 2001). Jones (2000) has reviewed what has been learnt from the first 5 years of this work. He finds it useful to divide the calculations that have been done into two categories which he calls *Busse-Zhang* (BZ) and *Glatzmaier-Roberts* (GR) models. The distinction is made according to the choice of the key parameters q, $\widetilde{\mathrm{Ra}}$ and E. BZ calculations typically have $\widetilde{\mathrm{Ra}}$ a few times $\widetilde{\mathrm{Ra}}_{c0}$ (the critical value for the onset of convection in the rapidly rotating system in the absence of any magnetic field), $\mathrm{q} \sim 10$ and $10^{-4} \leq \mathrm{E} \leq 10^{-3}$. They are characterised by velocities having magnitude of $O(10)$ on the thermal diffusion timescale [so the magnetic Reynolds number $\mathrm{Rm} = O(100)$, sufficient for dynamo action]. The magnetic field has only a weak influence on convection which takes place mostly outside the tangent cylinder. There is no strong differential rotation, poloidal and toroidal fields are comparable in magnitude and the dynamo can be thought of as of α^2 type. GR calculations are more supercritical with $\widetilde{\mathrm{Ra}} \sim 100\widetilde{\mathrm{Ra}}_{c0}$ and therefore much more computationally intensive. (Consequently most published work is in the BZ regime.) The larger $\widetilde{\mathrm{Ra}}$ is permitted by going to lower E. (Increasing $\widetilde{\mathrm{Ra}}$ at fixed E can result in dynamo action shutting off.) Convective velocities are larger, permitting lower values of q. There is a stronger differential rotation and the dynamo is more of $\alpha\omega$ type, although the peak poloidal field strength remains comparable with the that of the toroidal field.

Most of the work described above is for what Jones (2000) refers to as the "zero-order model", that is a spherically symmetric Boussinesq basic state with only one buoyancy source. The main exception is the work by Glatzmaier & Roberts (1996a,b,c) (and their subsequent papers) which use the anelastic approximation and both thermal and compositional buoyancy. Even within the zero-order model there is considerable scope for variation. As well as choice of the key governing parameters q, E, E_m and $\widetilde{\mathrm{Ra}}$ models differ in:

- *Inner core.* Most models include an inner core of radius about one third of that of the outer core with an electrical conductivity comparable with (and usually the same as) that of the outer core. Some have no inner core while others choose an insulating or perfectly conducting inner core. Wicht (2002) has recently concluded that in his model, the inner core does not play an important role in Earth-like reversal sequences.

- *Buoyancy distribution.* Even with thermal buoyancy only, there is scope to choose differential heating, internal heating or some combination of the two.

- *Inertia.* Its size is determined by the choice of E_m. Some models neglect it altogether ($\mathrm{E}_m = 0$) while others include it partially, for example only the axisymmetric azimuthal part important for the geostrophic flow.

- *Boundary conditions.* The values of E that we are forced to use in order to give a numerically tractable problem mean that the role of viscosity is significantly ampli-

fied compared with the real Earth. Kuang & Bloxham (1997, 1999) have applied stress-free boundary conditions, arguing that this reduces somewhat the influence of viscosity, in partial compensation for the effect of the larger Ekman number. Most calculations continue to apply rigid boundary conditions on $\mathbf{u}$.

Beyond the zero-order model, there have been several developments:

- *Density.* As mentioned above, Glatzmaier & Roberts (1996a,b,c, 1997, 1998) have championed the use of the anelastic approximation and of both thermal and compositional buoyancy. Their's is the only model that deals with the sources of buoyancy (mostly at the ICB) in a fully consistent manner, directly linking them to cooling at the CMB.

- *Heterogeneous boundary conditions.* The heat flow across the CMB is not spherically symmetric. Motivated by this, several groups have investigated the effect of heterogeneous thermal boundary conditions at the CMB. Glatzmaier *et al.* (1999) have shown the strong influence the choice of boundary condition has on reversal frequency. Olson & Christensen (2002) find that "When the amplitude of the boundary heat flow heterogeneity exceeds the average heat flow, the dynamos usually fail" and also find similarities between the present field and that produced by a model with boundary heat flow derived from lower-mantle seismic tomography, see also Christensen & Olson (2003). Bloxham (2000) compares the secular variation in the Kuang & Bloxham (1997, 1999) model with the paleomagnetic secular variation. He finds that, while there is a fair agreement for the meridional distribution, the amplitude in the numerical simulations is smaller by a factor of at least two. When he includes heterogeneous CMB heat flow in the model, he finds that he can match the amplitude of the paleomagnetic secular variation .

As computer power has increased and more groups have constructed their own models, a large number of model variations has been studied and several groups have undertaken parameter surveys (for example Christensen *et al.* 1999, Kutzner & Christensen 2002, Morrison & Fearn 2000, Fearn & Morrison 2001, Simitev & Busse 2002, 2003).

6 Where are we now, and the future

Our knowledge of the geomagnetic field comes from a number of distinct sources:

- *Paleomagnetic measurements.* These give the long-time behaviour; showing that the field is maintained on times very much longer than τ_η and give information about reversals, excursions, and the long-term secular variation. For example, in analyses of paleomagnetic data, Love (2000a) finds an inverse correlation between angular secular variation and field strength and Love (2000b) confirms the statistical significance of the paths taken by the virtual geomagnetic pole (VGP) during reversals having preferred locations.

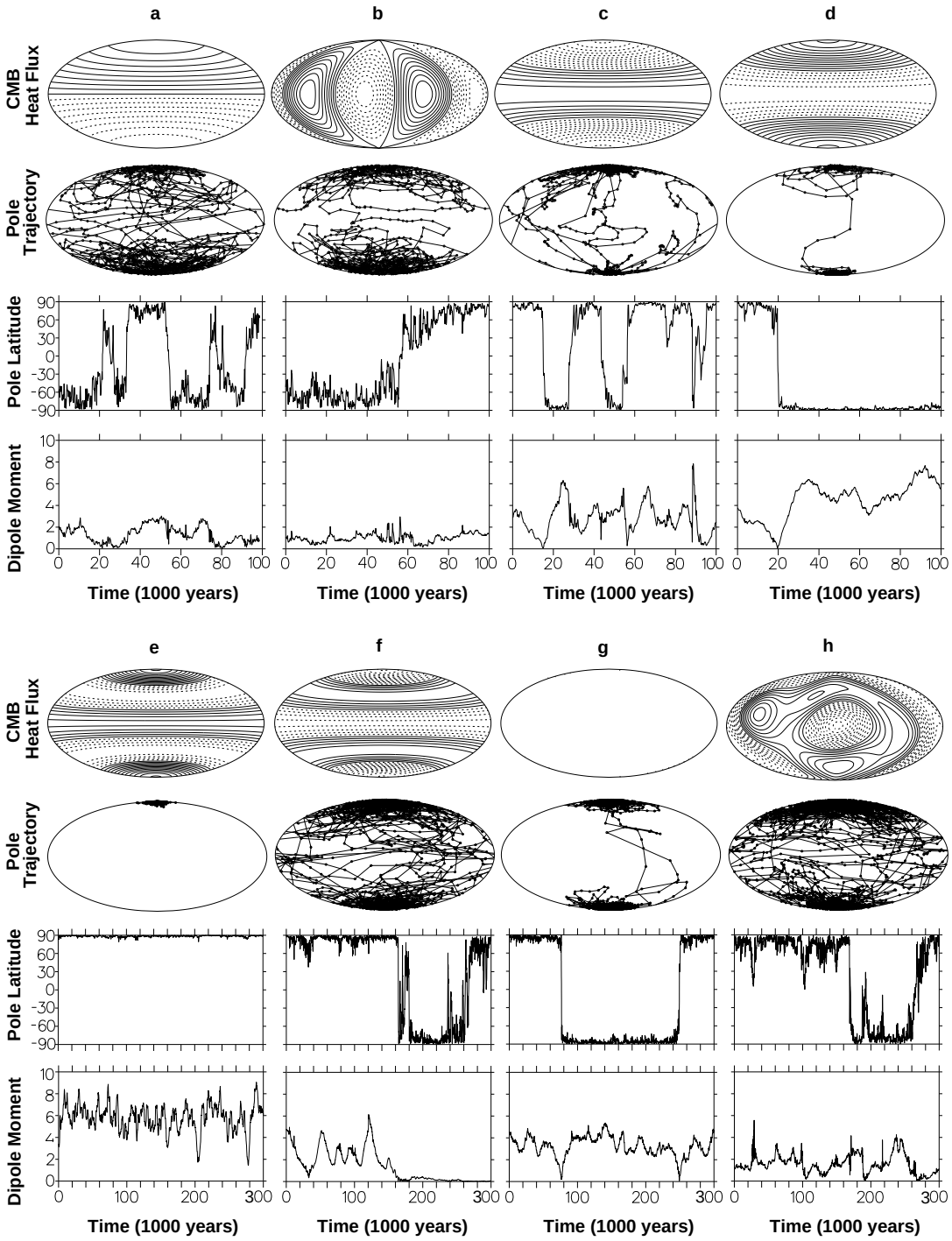

Figure 5: An example of the influence heterogeneous heat flux boundary conditions on the reversal behaviour of a dynamo model. From Glatzmaier *et al.* (1999

- *Surface observations.* These are available for about the past 400 years. Early measurements giving global coverage were largely made from ships. More recently a network of land-based observatories has provided good quality data.

- *Satellite observations.* The high quality data from MAGSAT (1979-1980) is now being complemented by ØRSTED allowing detailed models of the field and the secular variation over the past 20 years, see for example Hulot *et al.* (2002) and Jackson (2003).

In addition, there are other sources of information relevant to geodynamo simulations:

- *Seismological measurements.* In addition to giving vital information on the structure and composition of the core, recent work has used the anisotropy of the inner core to determine its rotation rate, see for example Tromp (2001).

There are two clear distinct aims in geodynamo modelling:

1. to understand the key physical processes of convection-driven hydrodynamic dynamos in parameter regimes characteristic of the Earth, and

2. to try to explain specific features of the observed geomagnetic field.

An example of [1] is to demonstrate the maintenance of a magnetic field of strength comparable with that of the Earth over times long compared with τ_η. An example of [2] is to explain the observed variation in the reversal frequency. We can expect that simpler models such as the zero-order models to be adequate for [1] while features specific to the Earth such as its heterogeneous CMB heat flow and its thermal history resulting in its inner-core growth to be necessary for [2]. Ultimately, we may hope to learn new facts about the interior of the Earth by matching the results of sophisticated modelling to observations.

Numerical simulations give reasonable results for the morphology and strength of the field at the CMB, and the models are also capable of giving reversals and excursions which can be compared with palaeomagnetic observations. They also predict differential rotation between the inner core and the mantle. Given the parameter values we are able to use, particularly for E and q, the success of our models is better than we might expect. Jones (2000) comments "The parameter regime in which the current generation of numerical models can be run is very far from the regime of geophysical parameter values; so far, indeed, that the strong similarity between the model outputs and the geodynamo is quite surprising."

We can expect progress in a number of directions in the coming years. Increasing computing power and improved numerical methods such as the inclusion of subgrid-scale models (see for example Buffett 2003 and Chapter **??**) should benefit all classes of models. Improved data and its analysis will identify generic and specific features of the Earth's field requiring explanation, motivating further developments away from the zero-order model.

Acknowledgements

Thanks are due to Paul Roberts who provided some very useful comments on an earlier version of this article. Thanks also to the authors who have given permission for their figures to be used. Credits are given in the figure captions.

References

Abramowitz M. & Stegun I.A. *Handbook of Mathematical Functions*, Dover, New York (1965).

Acheson D.J., *Elementary Fluid Dynamics*, Oxford University Press (1990).

Aldridge K., Dynamics of the core at short periods: theory, experiments and observations, in *Earth's core and lower mantle* (C.A. Jones, A.M. Soward & K. Zhang, eds.), Taylor and Francis, London, 180-210 (2003).

Alfè D., Gillan M.J., & Price G.D., Composition and temperature of the Earth's core constrained by combining *ab initio* calculations and seismic data, *Earth Planet. Sci. Lett.* **195**, 91-98 (2002a).

Alfè D., Gillan M.J., Vočadlo L., Brodholt, J. & Price G.D., The *ab initio* simulation of the Earths core, *Phil. Trans. R. Soc. Lond Ser. A* **360**, 1227-1244 (2002b).

Anderson O.L., The power balance at the core-mantle boundary, *Phys. Earth Planet. Inter.* **131**, 1-17 (2002).

Anderson O.L. & Isaak D.G., Another look at the core density deficit of Earth's outer core, *Phys. Earth Planet. Inter.* **131**, 19-27 (2002).

Backus G., Parker R. & Constable C., *Foundations of Geomagnetism*, Cambridge University Press (1996).

Batchelor G.K., *An Introduction to Fluid Dynamics*, Cambridge University Press (1967).

Barenghi C.F., Nonlinear planetary dynamos in a rotating spherical shell. II. The post-Taylor equilibration for α^2-dynamos, *Geophys. Astrophys. Fluid Dynam.* **67**, 27-36 (1992).

Bloxham J., The effect of thermal core-mantle interactions on the palaeomagnetic secular variation, *Phil. Trans. R. Soc. Lond Ser. A* **358**, 1171-1179 (2000).

Bloxham J. & Jackson A., Time-dependent mapping of the magnetic field at the core-mantle boundary, *J. Geophys. Res.* **97**, 19537-19563 (1992).

Bloxham J., Zatman S. & Dumberry M., The origin of geomagnetic jerks, *Nature* **420**, 65-68 (2002).

Bolt B.A., *Inside the Earth*, Freeman, San Fransisco (1982).

Braginsky S.I., Structure of the F layer and reasons for convection in the Earth's core, *Sov. Phys. Dokl.* **149**, 8-10 (1963).

Braginsky S.I., Torsional magnetohydrodynamic vibrations in the Earth's core and variations in day length, *Geomag. Aeron.* **10**, 1-8 (1970).

Braginsky S.I., Nearly axially symmetric model of the hydromagnetic dynamo of the Earth. I, *Geomag. Aeron.* **15**, 122-128 (1975).

Braginsky S.I., The nonlinear dynamo and model-Z, in *Lectures on Solar and Planetary Dynamos* (Proctor M.R.E. & Gilbert A.D., eds.) Cambridge University Press, 267-304 (1994).

Braginsky S.I. & Roberts P.H., A model-Z geodynamo, *Geophys. Astrophys. Fluid Dynam.* **38**, 327-349 (1987).

Braginsky S.I. & Roberts P.H., Equations governing convection in Earth's core and the geodynamo, *Geophys. Astrophys. Fluid Dynam.* **79**, 1-97 (1995).

Buffet B.A., A comparison of subgrid-scale models for large-eddy simulations of convection in the Earth's core, *Geophys. J. Int.* **153**, 753-765 (2003).

Busse F.H., Convective flows in rapidly rotating spheres and their dynamo action, *Phys. Fluids* **14**, 1301-1314 (2002).

Busse F.H., Grote E. & Simitev R., Convection in rotating spherical shells and its dynamo action, in *Earth's core and lower mantle* (C.A. Jones, A.M. Soward & K. Zhang, eds.), Taylor and Francis, London, 130-152 (2003).

Christensen U.R., Aubert J., Cardin P., Dormy E., Gibbons S., Glatzmaier G.A., Grote E., Honkura Y., Jones C., Kono M., Matsushima M., Sakuraba A., Takahashi F., Tilgner A., Wicht J. & Zhang K., A numerical dynamo benchmark, *Phys. Earth Planet. Inter.* **128**, 25-34 (2001).

Christensen U.R. & Olson P., Secular variation in numerical geodynamo models with lateral variations of boundary heat flow, *Phys. Earth Planet. Inter.* **138**, 39-54 (2003)

Christensen U., Olson P. & Glatzmaier G.A., Numerical modelling of the geodynamo: a systematic parameter survey, *Geophys. J. Int.* **138**, 393-409 (1999).

Courtillot V. & Le Mouël J.-L., Time variations of the Earth's magnetic field: from daily to secular, *Ann. Rev. Earth Planet. Sci.* **16**, 389-476 (1988).

de Wijs G.A., Kresse G., Vočadlo L., Dobson D., Alfè D., Gillan M.J. & Price G.D., The viscosity of liquid iron at the physical conditions of the Earth's core, *Nature* **392**, 805-807 (1998).

Dormy E., Valet J.-P. & Courtillot V., Numerical models of the geodynamo and observational constraints, *Geochem. Geophys. Geosyst.* **1**, paper number 2000GC000062 (2000).

Fearn D.R., Nonlinear planetary dynamos, in *Lectures on Solar and Planetary Dynamos* (Proctor M.R.E. & Gilbert A.D., eds.), CUP, 219-244 (1994).

Fearn D.R., Hydromagnetic flow in planetary cores, *Rep. Prog. Phys.* **61**, 175-235 (1998).

Fearn D. R. & Morrison G., The role of inertia in hydrodynamic models of the geodynamo, *Phys. Earth Planet. Inter.* **128**, 75-92 (2001).

Fearn D.R. & Proctor M.R.E., The stabilising role of differential rotation on hydromagnetic waves, *J. Fluid Mech.* **128**, 21-36 (1983).

Fearn D.R. & Proctor M.R.E., Dynamically consistent magnetic fields produced by differential rotation, *J. Fluid Mech.* **178**, 521-534 (1987).

Fearn D.R. & Proctor M.R.E., Magnetostrophic balance in non-axisymmetric, non-standard dynamo models, *Geophys. Astrophys. Fluid Dynam.* **67**, 117-128 (1992).

Fearn D.R. & Rahman M.M., Instability of nonlinear α^2-dynamos, *Phys. Earth Planet. Inter.* **142**, 101-112(2004a).

Fearn D.R. & Rahman M.M., The role of inertia in models of the geodynamo, *Geophys. J. Int.* **158**, 515-528 (2004b).

Fotheringham P., Fearn D.R. & Hollerbach R., Magnetic stability and nonlinear evolution of a selection of mean field dynamos. *Phys. Earth Planet. Inter.* **134**, 213-237 (2002).

Glatzmaier G.A., Geodynamo simulations - How realistic are they?, *Ann. Rev. Earth Planet. Sci.* **30**, 237-257 (2002).

Glazmaier G. A., Coe R. S., Hongre L. & Roberts, P. H., The role of the earth's mantle in controlling the frequency of geomagnetic reversals, *Nature* **401**, 885-890 (1999).

Glatzmaier G.A. & Roberts P.H., A three-dimensional self-consistent computer simulation of a

geomagnetic field reversal, *Nature* **377**, 203-209 (1995a).

Glatzmaier G.A. & Roberts P.H., A three-dimensional convective dynamo solution with rotating and finitely conducting inner core and mantle, *Phys. Earth Planet. Inter.* **91**, 63-75 (1995b).

Glatzmaier G.A. & Roberts P.H., On the magnetic sounding of planetary interiors, *Phys. Earth Planet. Inter.* **98**, 207-220 (1996a).

Glatzmaier G.A. & Roberts P.H., An anelastic evolutionary geodynamo simulation driven by compositional and thermal convection, *Physica D* **97**, 81-94 (1996b).

Glatzmaier G.A. & Roberts P.H., Rotation and magnetism of Earth's inner core, *Science* **274**, 1887-1891 (1996c).

Glatzmaier G.A. & Roberts P.H., Simulating the geodynamo, *Contemp. Phys.* **38**, 269-288 (1997).

Glatzmaier G.A. & Roberts P.H., Dynamo theory then and now, *Int. J. Eng. Sci.* **36**, 1325-1338 (1998).

Glatzmaier G.A., Coe R.S., Hongre L. & Roberts P.H., The role of the Earth's mantle in controlling the frequency of geomagnetic reversals, *Nature* **401**, 885-890 (1999).

Gubbins D., The distinction between geomagnetic excursions and reversals, *Geophys. J. Int.* **197**, F1-F3(1999).

Gubbins D., The Rayleigh number for convection in the Earths core, *Phys. Earth Planet. Inter.* **128**, 312 (2001).

Gubbins D., Alfè D., Masters G., Price D. & Gillan M.J., Can the Earth's dynamo run on heat alone?, *Geophys. J. Int.* **155**, 609-622 (2003).

Gubbins D., Alfè D., Masters G., Price D. & Gillan M.J., Gross thermodynamics of 2-component core convection, *Geophys. J. Int.* **157**, 1407-1414 (2004).

Heller R., Merrill R.T. & McFadden P.L., The variation of the intensity of the earth's magnetic field with time, *Phys. Earth Planet. Inter.* **131**, 237-249.

Hollerbach R., A spectral solution of the magneto-convection equations in spherical geometry, *Int. J. Num. Meth. Fluids* **32**, 773-797 (2000).

Hollerbach R. & Ierley G., A modal α^2-dynamo in the limit of asymptotically small viscosity, *Geophys. Astrophys. Fluid Dynam.* **56**, 133-158 (1991).

Hollerbach R. & Jones C.A., A geodynamo model incorporating a finitely conducting inner core, *Phys. Earth Planet. Inter.* **75**, 317-327 (1993).

Hollerbach R. & Jones C.A., On the magnetically stabilising role of the Earth's inner core, *Phys. Earth Planet. Inter.* **87**, 171-181 (1995).

Hulot G., Eymin C., Langlais B., Mandea M. & Olsen N., Small-scale structure of the geodynamo inferred from Oersted and Magsat satellite data, *Nature* **416**, 620-623 (2002).

Jackson A., Intense equatorial flux spots on the surface of the Earths core, *Nature* **424**, 760-763 (2003).

Jackson A., Jonkers A.R. & Walker M.R., Four centuries of geomagnetic secular variation from historical records, *Phil. Trans. R. Soc. Lond Ser. A* **358**, 957-990 (2000).

Jault D., Model Z by computation and Taylor's condition, *Geophys. Astrophys. Fluid Dynam.* **79**, 99-124 (1995).

Jault D., Electromagnetic and topographic coupling, and LOD variations, in *Earth's core and lower mantle* (C.A. Jones, A.M. Soward & K. Zhang, eds.), Taylor and Francis, London, 56-76 (2003).

Jault D. & Le Mouël J.-L., Exchange of angular momentum between the core and the mantle, *J. Geomag. Geoelectr.* **43**, 111-129 (1991).

Jones C.A., Convection-driven geodynamo models, *Phil. Trans. R. Soc. Lond Ser. A* **358**, 873-897 (2000).

Jones C.A., Longbottom A.W. & Hollerbach, R., A self-consistent convection driven geodynamo model, using a mean field approximation, *Phys. Earth Planet. Inter.* **92**, 119-141 (1995).

Kono M. & Roberts P.H., Recent geodynamo simulations and observations of the geomagnetic field, *Rev. Geophys.* **40**, art. no. 1013 (2002).

Kono M. & Tanaka H., Intensity of the geomagnetic field in geological time: A statistical study, in *The Earth's Central Part: Its Structure and Dynamics* (T. Yukutake, ed.), pp. 75-94, Terrapub, Tokyo (1995).

Kuang, W. & Bloxham J., An Earth-like numerical dynamo model, *Nature* **389**, 371-374 (1997).

Kuang, W. & Bloxham J., Numerical modelling of magnetohydrodynamic convection in a rapidly rotating spherical shell: weak and strong field dynamo action, *J. Comp. Phys.* **153**, 51-81 (1999).

Kutzner C. & Christensen U.R., From stable dipolar towards reversing numerical dynamos, *Phys. Earth Planet. Inter.* **131**, 29-45 (2002).

Labrosse S., Poirier J.-P. & LeMouel J.-L., The age of the inner core, *Earth Planet. Sci. Lett.* **190**, 111-123 (2001).

Loper D. E. & Roberts P. H., Compositional convection and the gravitationally powered dynamo, in *Stellar and Planetary Magnetism* (A. M. Soward, ed.), Gordon and Breach, New York, 297-327 (1983).

Love J., Palaeomagnetic secular variation as a function of intensity, *Phil. Trans. R. Soc. Lond Ser. A* **358**, 1191-1223 (2000a).

Love J., Statistical assessment of preferred transitional VGP longitudes based on palaeomagnetic lava data, *Geophys. J. Int.* **140**, 211-221 (2000b).

McFadden P.L. & Merrill R.T., Inhibition and geomagnetic field reversals, *J. Geophys. Res.* **98**, 6189-6199 (1993).

McFadden P.L. & Merrill R.T., Evolution of the geomagnetic reversal rate since 160Ma: Is the process continuous?, *J. Geophys. Res.* **105**, 28455-28460 (2000).

Malkus W.V.R., Energy sources for planetary dynamos, in *L*ectures on Solar and Planetary Dynamos (Proctor M.R.E. & Gilbert A.D., eds.) Cambridge University Press, 161-179 (1994).

Malkus W.V.R. & Proctor M. R. E., The macrodynamics of α-effect dynamos in rotating fluids, *J. Fluid Mech.* **67**, 417-443 (1975).

Melchior P.J., *T*he physics of the Earth's core, Pergamon, Oxford (1986).

Merrill R.T., McElhinney M.W. & McFadden P.L., *The Magnetic Field of the Earth: Paleomagnetism, the Core, and the Deep Mantle*, Academic Press (1996).

Merrill R.T. & McFadden P.L., The geomagnetic axial dipole field assumption, *Phys. Earth*

Planet. Inter. **139**, 171-185 (2003).

Moffatt H.K., 1978. *Magnetic Field Generation in Electrically Conducting Fluids*, Cambridge University Press (1978).

Morrison G & Fearn D.R., The infuence of Rayleigh number, azimuthal wavenumber and inner core radius on $2\frac{1}{2}$D hydromagnetic dynamos, *Phys. Earth Planet. Inter.* **112**, 237-258 (2000).

Olson P., Thermal interaction of the core and mantle, in *Earth's core and lower mantle* (C.A. Jones, A.M. Soward & K. Zhang, eds.), Taylor and Francis, London, 1-38 (2003).

Olson P. & Christensen U.R., The time-averaged magnetic field in numerical dynamos with non-uniform boundary heat flow, *Geophys. J. Int.* **151**, 809-823 (2002).

Pais A. & Hulot G., Length of day decade variations, torsional oscillations and inner core super-rotation: evidence from recovered core surface zonal flows, *Phys. Earth Planet. Inter.* **118**, 291316 (2000).

Poirier J.-P., *Introduction to the Physics of the Earths Interior*, Cambridge University Press, Cambridge, UK (2000).

Proctor M. R. E., Numerical solutions of the nonlinear α-effect dynamo equations, *J. Fluid Mech.* **80**, 769-784 (1977).

Proctor M.R.E., Convection and magnetoconvection in a rapidly rotating sphere, in *Lectures on Solar and Planetary Dynamos* (Proctor M.R.E. & Gilbert A.D., eds.) Cambridge University Press, 1-58 (1994).

Roberts P.H., From Taylor state to model-Z ?, *Geophys. Astrophys. Fluid Dynam.* **49**, 143-160 (1989).

Roberts P.H., Fundamentals of dynamo theory, in *Lectures on Solar and Planetary Dynamos* (Proctor M.R.E. & Gilbert A.D., eds.) Cambridge University Press, 1-58 (1994).

Roberts P.H. & Glatzmaier G.A., Geodynamo theory and simulations, *Rev. Mod. Phys.* **72**, 1081-1123 (2000).

Roberts P.H., Jones C.A. & Calderwood A.R., Energy fluxes and ohmic dissipation in the Earth's core, in *Earth's core and lower mantle* (C.A. Jones, A.M. Soward & K. Zhang, eds.), Taylor and Francis, London, 100-129 (2003).

Roberts P.H. & Soward A.M., Magnetohydrodynamics of the Earth's core, *Ann. Rev. Fluid Mech.* **4**, 117-154 (1972).

Roberts P.H. & Soward A.M., *Rotating Fluids in Geophysics*, Academic Press, London (1978).

Rotvig J. & Jones C.A., Rotating convection-driven dynamos at low Ekman number, *Phys. Rev. E* **66**, 056308:1-15(2002).

Sakuraba A. & Kono M., Effect of the inner core on the numerical solution of the magnetohydrodynamic dynamo, *Phys. Earth Planet. Inter.* **111**, 105-121 (1999).

Sarson G.R., Reversal models from dynamo calculations, *Phil. Trans. R. Soc. Lond Ser. A* **358**, 921-942 (2000).

Sarson G.R. & Jones C.A., A convection driven geodynamo reversal model, *Phys. Earth Planet. Inter.* **111**, 3-20 (1999).

Sarson G.R., Jones C.A. & Longbottom A.W., The influence of boundary region heterogeneities on the geodynamo, *Phys. Earth Planet. Inter.* **101**, 13-32 (1997).

Sarson G.R., Jones C.A. & Longbottom A.W., Convection driven geodynamo models of varying Ekman number, *Geophys. Astrophys. Fluid Dynam.* **88**, 225-259 (1998).

Schubert G. & Zhang K. Effects of an electrically conducting inner core on planetary and stellar dynamos, *Ap. J.* **557**, 930-942 (2001).

Simitev R., & Busse F.H., Parameter dependences of convection driven spherical dynamos, in *High performance computing in science and engineering* (E. Krause & W. Jager, eds), Springer-Verlag, Heidelberg (2002).

Simitev R., & Busse F.H., Low Prandtl number convection in rotating spherical fluid shells and its dynamo states, in *High performance computing in science and engineering* (E. Krause & W. Jager, eds), Springer-Verlag, Heidelberg (2003).

Skinner P.H. & Soward A.M., Convection in a rotating magnetic system and Taylor's constraint, *Geophys. Astrophys. Fluid Dynam.* **44**, 91-116 (1988).

Skinner P.H. & Soward A.M., Convection in a rotating magnetic system and Taylor's constraint II. *Geophys. Astrophys. Fluid Dynam.* **60**, 335-356 (1990).

Soward A.M., Non-linear marginal convection in a rotating magnetic system, *Geophys. Astrophys. Fluid Dynam.* **35** 329-371 (1986).

Soward A.M. & Jones C.A., α^2-dynamos and Taylor's constraint, *Geophys. Astrophys. Fluid Dynam.* **27**, 87-122 (1983).

Soward A.M. & Hollerbach R., Non-axisymmetric magnetohydrodynamic shear layers in a rotating spherical shell, *J. Fluid Mech.* **408**, 239-274 (2000).

Stacey F.D. *Physics of the Earth, 3rd ed.* Brisbane, Brookfield, 513pp, (1992).

Stern D.P., A Millennium of Geomagnetism, *Rev. Geophys.*, **40**(3), p.1-1 to 1-30, (2002) (see `http://www-spof.gsfc.nasa.gov/earthmag/mill_1.htm`).

Taylor J.B., The magnetohydrodynamics of a rotating fluid and the Earth's dynamo problem, *Proc. R. Soc. Lond Ser. A* **274**, 274-283 (1963).

Tromp J., Inner-core anisotropy and rotation, *Ann. Rev. Earth Planet. Sci.* **29**, 47-69 (2001).

Verhoogen J., Heat balance of the Earth's core, *Geophys. J. R. Astr. Soc.***4**, 276-281 (1961).

Verhoogen J., *E*nergetics of the Earth, National Academy Press Washington D.C. (1980).

Walker M.R., Barenghi C.F. & Jones C.A., A note on dynamo action at asymptotically small Ekman number, *Geophys. Astrophys. Fluid Dynam.* **88**, 261-275 (1998).

Wicht K., Inner-core conductivity in numerical dynamo simulations, *Phys. Earth Planet. Inter.* **132**, 281302 (2002).

Zhang K. & Busse F.H., Convection driven magnetohydrodynamic dynamos in rotating spherical shells, *Geophys. Astrophys. Fluid Dynam.* **49**, 97-116 (1989).

Zhang K. & Busse F.H., Generation of magnetic fields by convection in a rotating spherical fluid shell of infinite Prandtl number, *Phys. Earth Planet. Inter.* **59**, 208-222 (1990).

Zhang K. & Gubbins D., Is the geodynamo process intrinsically unstable?, *Geophys. J. Int.* **140**, F1-F4 (2000).

Zhang K. & Jones C.A., On small Roberts number magnetoconvection in rapidly rotating systems, *Proc. R. Soc. Lond Ser. A* **452**, 981-995 (1996).

Zhang K. & Jones C.A., The effect of hyperviscosity on geodynamo models, *Geophys. Res. Lett.*

24, 2869-2872 (1997).